Communication

Capturing the Moment of Emergence of Crystal Nucleus from Disorder

Takayuki Nakamuro, Masaya Sakakibara, Hiroki Nada, Koji Harano, and Eiichi Nakamura*

Cite This: https://dx.doi.org/10.1021/jacs.0c12100

Read Online

ACCESS | 📊 Metrics & More | 📰 Article Recommendations | 🆂🅸 Supporting Information

ABSTRACT: Crystallization is the process of atoms or molecules forming an organized solid via nucleation and growth. Being intrinsically stochastic, the research at an atomistic level has been a huge experimental challenge. We report herein in situ detection of a crystal nucleus forming during nucleation/growth of a NaCl nanocrystal, as video recorded in the interior of a vibrating conical carbon nanotube at 20−40 ms frame^{-1} with localization precision of <0.1 nm. We saw NaCl units assembled to form a cluster fluctuating between featureless and semiordered states, which suddenly formed a crystal. Subsequent crystal growth at 298 K and shrinkage at 473 K took place also in a stochastic manner. Productive contributions of the graphitic surface and its mechanical vibration have been experimentally indicated.

Self-organization of atoms and molecules into crystals plays a key role in diverse areas of science and technology,[1] biology,[2,3] and the environment.[4] Crystallization occurs in two stages, nucleation and growth. Nucleation starts with a clustering of the constituents and phase transition at a saddle point of the potential energy surface[5,6] illustrated as a simple model in Figure 1a for homogeneous nucleation of NaCl in the gas phase.[7] As the size of a prenucleation cluster increases toward a critical radius r_c, there forms a critical nucleus—a transient species so far undetectable by experiments. Theory has suggested that the nucleation process seen at an atomistic or molecular level is stochastic,[8] like any chemical reactions analyzed at this level.[9] Atomistic experimental studies of the nucleation process have therefore been a huge challenge,[10−13] and it has remained largely the subject of theory,[14] simulation,[15] and mimicry.[16,17] A step forward in this challenge has recently been provided by isolation from a bulk solution and ex situ characterization of prenucleation clusters using single-molecule atomic-resolution real-time electron microscopy (SMART-EM).[18,19] We report herein in situ atomic-resolution detection of a crystal nucleus forming during nucleation/growth of a NaCl nanocrystal, which took place at 298 K in a few tens of nm^3 vacuum space of a vibrating conical carbon nanotube (CNT),[20] as recorded at 20−40 ms frame^{-1} with localization precision of <0.1 nm.[21] In a CNT at 298 K studied on a transmission electron microscope (TEM), the nucleation/growth took place nine times during 152 s (Figures 2 and 3). First, in the narrow apex region,[22] a few NaCl units gathered and grew to form a transient cluster with morphology fluctuating between featureless and semiordered states,[5] from which suddenly emerged a crystal nucleus over the nine times in a reproducible manner (Figure 2). The video images reveal that the two-step mechanism of crystal nucleation may include multiple nonproductive semiordered clusters forming before the final cluster that produces a crystalline nucleus (Figure 1d).[5] Homoepitaxial growth then took place stochastically as the crystal vibrated in the CNT.[8,23,24] At 473 K, a crystal was

found to shrink in a stochastic manner (Figure 4).[25] We anticipate that the SMART-EM setup[26] provides a versatile platform for studies of self-assembly and other chemical events in atomistic details so far unachievable.[27,28]

Unlike previous works using a molten inorganic salt that penetrates the entire interior of a narrow CNT,[29] we introduced aqueous NaCl into a CNT and removed water in vacuo to grow a nanocrystal in the void space (e.g., Figure 1b). To this end, we soaked a water-soluble aggregate of aminated conical CNTs (carbon nanohorns)[30] in saturated aq. NaCl at 25 °C for 24 h, dried it in vacuo (298 K, 0.5 h) and, upon TEM analysis, found a single nanometer-sized NaCl crystal in a CNT as also characterized by energy-dispersive X-ray spectroscopic analysis (Figure S2). The crystals were found in approximately 10% of the CNTs (no crystal found after 1 h immersion in aq. NaCl). Thus, the diffusion of aq. NaCl into the CNTs through an undetected structural defect is slow. The CNT vibrated stochastically several times per second with an amplitude of ± <0.1 nm (cf. Figure 1c, Figure S3, Movie S1),[21] and this mechanical vibration was essential for the observed crystal growth (see below).

Approximately 5% of several tens of NaCl crystals examined were held tightly in cylindrical CNTs (always one crystal in one CNT), and neither grew nor shrank during observation. Figure 1b shows an example of such stable crystals seen as a rectangular array of 40 dots, 20 NaCl units (denoted as (5,8) crystal). The interatomic distance of 0.273(16)−0.277(8) nm is slightly shorter than the distance of 0.2820(1) nm in a bulk crystal at 298 K[31] (Figure S4) as theoretically predicted.[32]
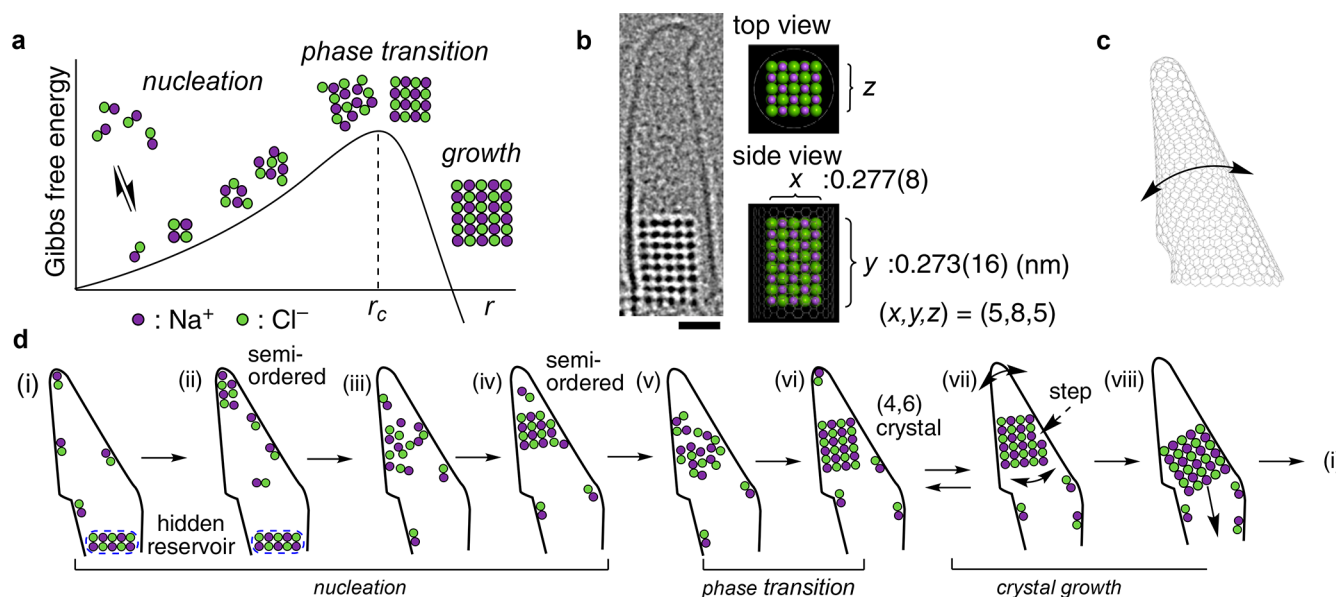
A

Figure 1. Nucleation and growth of a NaCl nanocrystal in a vibrating CNT. (a) Schematic energy diagram of crystallization. The radius of a critical nucleus shown as r_c. (b) TEM image of a NaCl nanocrystal at 298 K in an aminated CNT of a size denoted as (x, y, z) with x, y, and z (thickness) defined herein. Throughout this work, the assignment on which of Na$^+$ and Cl$^-$ occupies the corners of a crystal is arbitrary, because the TEM image lacks this information. The amino groups on CNT are too small to be seen. Scale bar 1 nm. Acceleration voltage 80 kV and electron dose rate of 3.6×10^5 e$^-$ nm^{-2} s^{-1}. Whenever necessary, the moiré pattern due to the graphitic lattice was removed by inverse fast Fourier transform (Figure 1 in Supporting Information Figure S1). (c) Model of a conical CNT shown with a curved arrow illustrating vibration. (d) Schematic diagram of the crystallization. NaCl molecules are supplied from a hidden reservoir. Vibrations of CNT and crystal are shown with curved arrows.

Note that the crystal packing of inorganic crystals grown from their molten salt in a CNT was strongly perturbed from the one in the corresponding bulk crystal.[29] The thickness (z) would be close to the width (x) because of the circular cross section of the CNT, minimization of surface energy ($x \approx y \approx z$), and neutrality of the crystal. Thus, the (5,8) crystal in Figure 1b would contain 100 NaCl units (i.e., (5,8,5) crystal). A preliminary gray value analysis, though the accuracy reduced by image blurring, indicated that the nanocrystals have a thickness of a few NaCl units, supporting the structure assignment stated above.[33]

The rest (95%) of the NaCl crystals were found in vibrating conical CNTs (cf. Figure 1c,d; Figure S5). In the conical CNTs, but not in the cylindrical ones, we made a striking observation—spontaneous crystal nucleation and growth taking place nine times at 298 K during 152 s (Figures 2 and 3). Figure 1d illustrates a rationale for the observed events. Based on an average crystal growth rate of 24.4 NaCl s^{-1} (Figure 2d), we consider that numerous neutral NaCl molecules translate back and forth in the CNT (the motions are too fast to be seen), and become trapped in the narrow and polarized conical apex.[22] Thus, in the beginning (ii), a short-lived semiordered cluster(s) made of several NaCl units forms, breaks down to a disordered cluster (iii), reorganizes into a larger semiordered cluster(s) (iv), and breaks down (v) until phase transition to a (4,6) crystal (vi). We consider that a (4,6) crystal is a (4,6,4) crystal comprising 48 NaCl units, in light of a report on a 48 NaCl cluster forming among a series of stable clusters of unassigned structures ((NaCl)$_n$, n = 18, 20, 24, 30, 32, 40, 48, 50, 56, 60, and 72 (Figure S6) upon quenching of a NaCl vapor at 300 K at 133 Pa).[34] The crystal then grows larger layer-by-layer as the CNT vibrates stochastically (vii, viii), and gradually moves toward the more spacious bottom part that can accommodate a larger crystal. This crystal supplies NaCl molecules in the next cycle (back to (i)). This

intriguing oscillation phenomenon suggests the presence of a thermal gradient created by the electron beam preferentially heating the CNT aggregates' interior.

Figure 2a shows four TEM snapshots in each of the nine events, on which we performed statistical analysis (Figure 2b–e). The event repeated nine times over 152 s until the specimen drifted away from the view frame. In all events, a small cluster appeared, grew, and produced a (4,6) crystal, which grew larger and disappeared into the bottom of the CNT (cf. fourth and eighth events), and the process started again after several seconds. Note that in all nine events, the crystals that appeared after (4,6) grew irreversibly, while the prenucleation clusters before (4,6) formed reversibly. Thus, the emergence of the (4,6) crystal nucleus marks the end of the nucleation period.

Figure 2b shows the duration of the nucleation period in red, and the period of the initial stage of growth in blue (growth from (4,6) to (6,8), or from 48 to 144 NaCl). We find similarity in the duration of the two periods in each event, but diversity among the nine events. Shown in Figure 2c, the nucleation period over the nine events roughly follows a normal distribution with an average time of 5.07 s, since the nucleation process produced the same (4,6) crystal every time. The growth period distributes more randomly because the growth process produced a different crystal every time. The growth period averages to be 3.94 s, which indicates 24.4 NaCl units incorporated every second into the crystal (Figure 2d). This property of the initial growth is supported by the stochastic growth pathways shown in Figure 2e. For example, the first event went through (4,6), (5,6), (5,7), (6,7), and (6,8) crystals, and the other eight events took different courses. Given the growth rate of 24.4 NaCl s^{-1}, we would expect that the nucleation period should have ended in 2 s instead of 5.07 s, indicating in turn the probabilistic nature of the nucleation process.
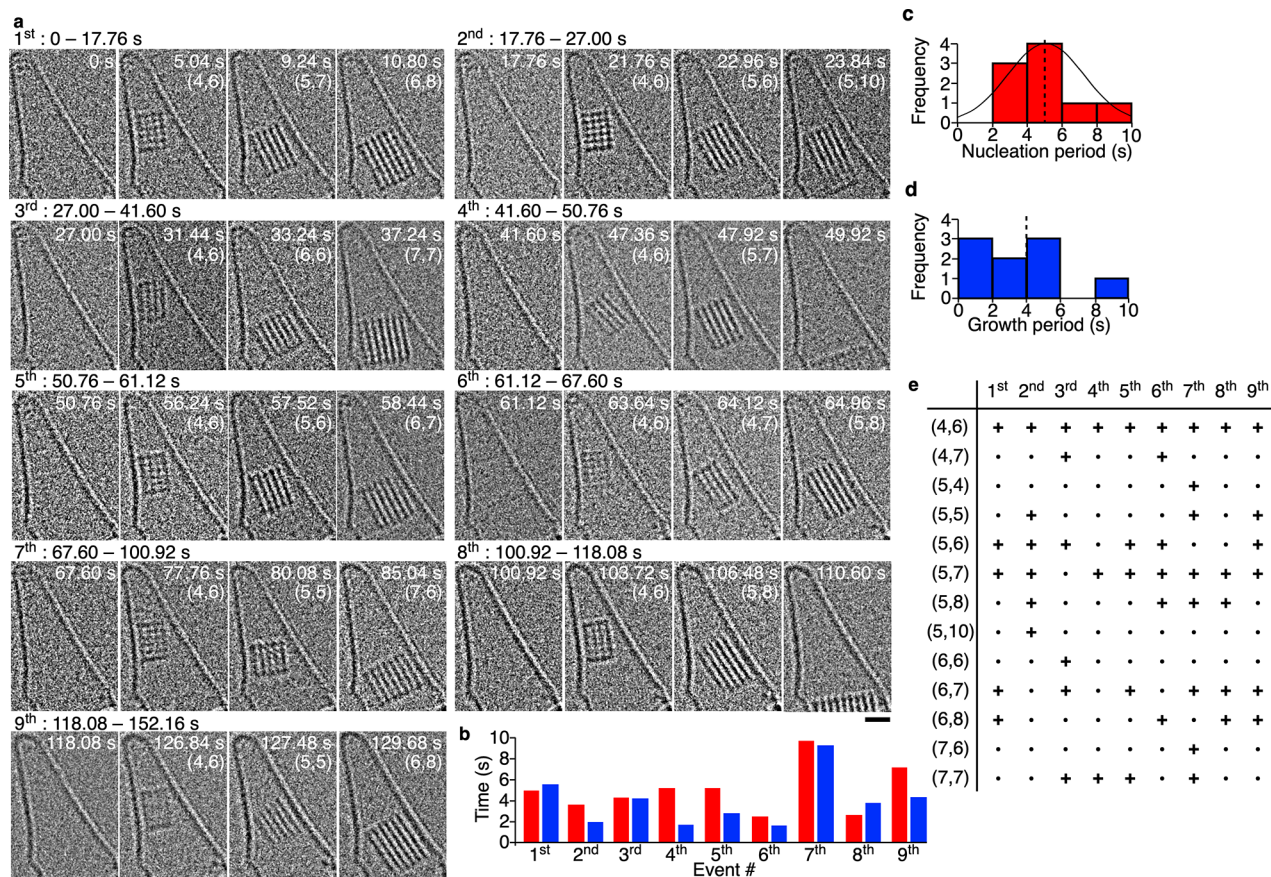
Figure 2. Nucleation/growth events taking place nine times. (a) Four representative snapshots in each event (40 ms frame^{-1}). Time 0 is the time when a NaCl cluster first appeared. The crystal size in parentheses. Acceleration voltage 80 kV and electron dose rate 4.0×10^5 e$^-$ nm^{-2} s^{-1} with small dose fluctuation (Figure S7). Scale bar 1 nm. The position of the images in each frame is normalized for the outline of the vibrating CNT (cf. Movies S1–S4). See Figure S8 for a 318-frame data set. (b) Histogram of the time until the appearance of a (4,6) crystal (red) and growth until (6,8) crystal or its size equivalent (blue). (c) Normal distribution of nucleation time period (black line) with an average of 5.07 s and standard deviation (sd) of 2.18 s. (d) Distribution of initial growth time period (average of 3.94 s and sd of 2.33 s), during which the crystal grew from 48 to 144 NaCl with a rate of 24.4 NaCl s^{-1}. (e) The course of the crystal growth in the nine events (column) and crystal sizes observed (+) during the growth (row).
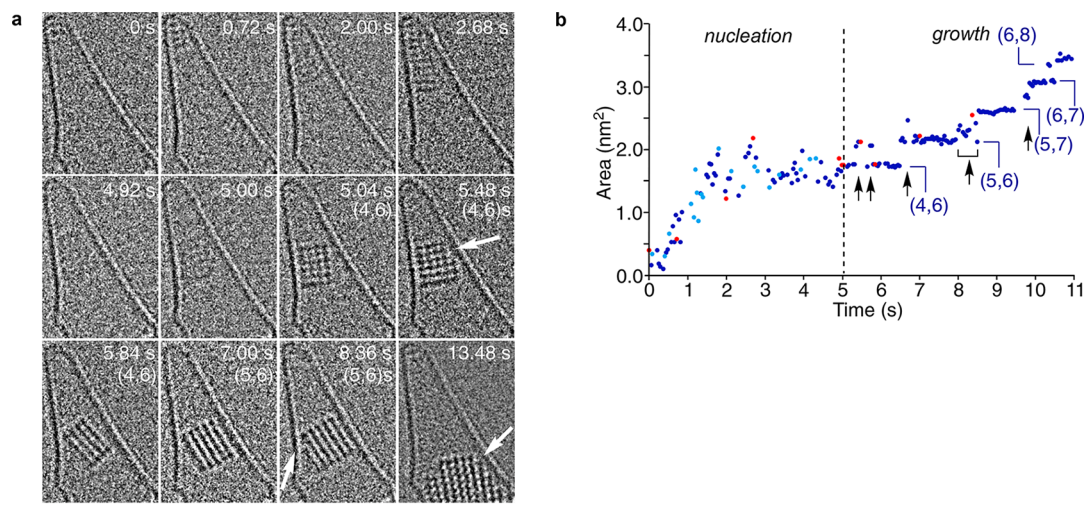

Figure 3. Nucleation/growth at 298 K. (a) Cluster/crystal images in the first event shown in Figure 2a. White arrows indicate steps in contact with the CNT wall. (b) Time evolution of 2-D area of cluster/crystal images. The nucleation phase ended at the dotted line at 5.04 s, before which featureless (light blue) and semiordered clusters (dark blue) alternately appeared. Arrows indicate step formation, and red dots the snapshots shown in (a).
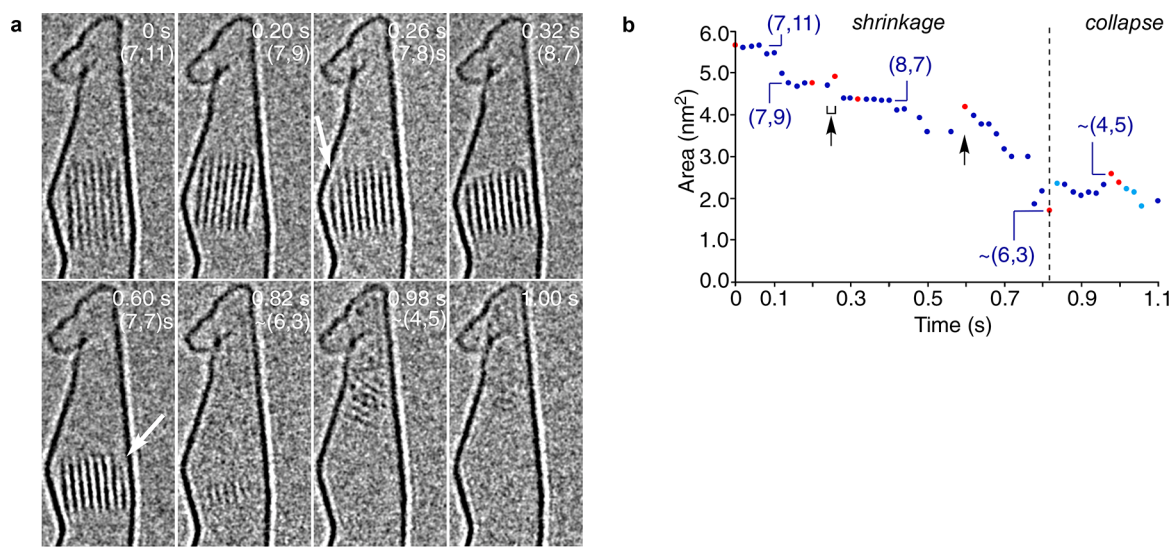
C

Figure 4. Shrinkage/collapse at 473 K. (a) Crystal shrinkage at 473 K (20 ms frame^{-1}). Time 0 is set arbitrarily. See Figure S10 and Movie S5 for a 28-frame data set. Scale bar 1 nm. (b) Time evolution of the 2-D area of the images with the dotted line showing the end of the shrinkage stage.

At 298 K, we saw exclusive crystal formation, and, at higher temperature, we saw crystal shrinkage. Figure 3 illustrates details of the first event of the nucleation/growth at 298 K shown in Figure 2a (Figure S9), and Figure 4 illustrates an example of the shrinkage at 473 K. In the initial 5 s of Figure 3a, featureless and semiordered morphology alternated before the formation of the (4,6) crystal at 5.04 s.[5,8] At 0−0.72 s, we saw a cluster growing up to approximately 2 × 3 in size near the apex that then disappeared quickly, and at 2.00−2.68 s, the appearance of a semiordered cluster made of several rows of NaCl along the graphitic wall, which also disappeared quickly. A sequence from 5.00 to 5.04 s is particularly noteworthy because a clear image of the (4,6) crystal nucleus suddenly emerged from a featureless object. Note that all of the semiordered prenucleation clusters before 5.04 s formed reversibly, while the crystals after 5.04 s grew irreversibly as found in the eight other events (cf. Figure S8). During the next 6 s, stochastic homoepitaxial growth of the (4,6) crystal occurred.[8,24] At 5.48 s, we saw the formation of a step in contact with the graphitic wall (arrow; (4,6)s with s denoting step), its disappearance to regenerate (4,6) in the next frame, and further growth to (5,6). As a note of caution, we assume that the crystal growth took place three-dimensionally, although the TEM information was limited to 2-D.

Finally, we examined the shrinkage of a NaCl crystal at 473 K. In a vibrating conical CNT, we found a NaCl crystal shrank in less than 1 s as shown in Figure 4a. A (7,11) crystal first shrank in a longitudinal direction into (7,9) (at 0.20 s) and gained width to form (8,7) to fit in a wider section of the CNT (0.32 s), which then shrank via step formation at 0.60 s into a crystal of a size approximately (6,3) at 0.82 s. The interatomic distance measured for the crystal between 0 and 0.82 s remained constant (0.278(4)−0.283(15) nm) until sudden collapse into a new crystal of an approximately (4,5) size (0.283(11)−0.285(6) nm) that we find in the tip of the CNT. The blurred lattice images often found in Figure 4a suggest dynamic defect formation during the degradation.

■ ASSOCIATED CONTENT

Ⓢ Supporting Information

The Supporting Information is available free of charge at https://pubs.acs.org/doi/10.1021/jacs.0c12100.

Methods and Materials and Representative TEM images (PDF)

Movie S1: Vibration of a conical CNT at 298 K (MOV

Movie S2: Nine times crystallization of NaCl in a conical CNT at 298 K (0−44.40 s) (MOV)

Movie S3: Nine times crystallization of NaCl in a conical CNT at 298 K (44.44−88.84 s) (MOV)

Movie S4: Nine times crystallization of NaCl in a conical CNT at 298 K (88.88−133.28 s) (MOV)

Movie S5: Shrinkage/collapse of NaCl in a conical CNT at 473 K (MOV)

■ AUTHOR INFORMATION

Corresponding Author

Eiichi Nakamura − *Department of Chemistry, The University of Tokyo, Tokyo 113-0033, Japan;* Ⓘ orcid.org/0000-0002-4192-1741; Email: nakamura@chem.s.u-tokyo.ac.jp

Authors

Takayuki Nakamuro − *Department of Chemistry, The University of Tokyo, Tokyo 113-0033, Japan;* Ⓘ orcid.org/0000-0002-0752-3475

Masaya Sakakibara − *Department of Chemistry, The University of Tokyo, Tokyo 113-0033, Japan*

Hiroki Nada − *Environmental Management Research Institute, National Institute of Advanced Industrial Science and Technology (AIST), Tsukuba 305-8569, Japan;* Ⓘ orcid.org/0000-0002-1744-2759

Koji Harano − *Department of Chemistry, The University of Tokyo, Tokyo 113-0033, Japan;* Ⓘ orcid.org/0000-0001-6800-8023

Complete contact information is available at:
https://pubs.acs.org/10.1021/jacs.0c12100

REFERENCES

(1) Mullin, J. W. *Crystallization*, 4th ed.; Butterworth Heinemann: Oxford, UK, 2001.

(2) (a) Wolde, P. R.; Frenkel, D. Enhancement of protein crystal nucleation by critical density fluctuations. *Science* **1997**, *277*, 1975−1978. (b) Dey, A.; Bomans, P. H. H.; Müller, F. A.; Will, J.; Frederik, P. M.; de With, G.; Sommerdijk, N. A. J. M. The role of prenucleation clusters in surface-induced calcium phosphate crystallization. *Nat. Mater.* **2010**, *9*, 1010−1014.

(3) (a) Sommerdijk, N. A. J. M.; de With, G. Biomimetic CaCO$_3$ mineralization using designer molecules and interfaces. *Chem. Rev.* **2008**, *108*, 4499−4550. (b) Pouget, E. M.; Bomans, P. H. H.; Goos, J. A. C. M.; Frederik, P. M.; de With, G.; Sommerdijk, N. A. J. M. The initial stages of template-controlled CaCO$_3$ formation revealed by cryo-TEM. *Science* **2009**, *323*, 1455−1458.

(4) Bartels-Rausch, T. Ten things we need to know about ice and snow. *Nature* **2013**, *494*, 27−29.

(5) (a) Vekilov, P. G. Nucleation. *Cryst. Growth Des.* **2010**, *10*, 5007−5019. (b) Nielsen, M. H.; Aloni, S.; De Yoreo, J. J. In situ TEM imaging of CaCO$_3$ nucleation reveals coexistence of direct and indirect pathways. *Science* **2014**, *345*, 1158−1162.

(6) (a) Erdemir, D.; Lee, A. Y.; Myerson, A. S. Nucleation of crystals from solution: Classical and two-step models. *Acc. Chem. Res.* **2009**, *42*, 621−629. (b) De Yoreo, J. J.; Gilbert, P. U. P. A.; Sommerdijk, N. A. J. M.; Penn, R. L.; Whitelam, S.; Joester, D.; Zhang, H.; Rimer, J. D.; Navrotsky, A.; Banfield, J. F.; Wallace, A. F.; Michel, F. M.; Meldrum, F. C.; Cölfen, H.; Dove, P. M. Crystallization by particle attachment in synthetic, biogenic, and geologic environments. *Science* **2015**, *349*, aaa6760.

(7) Kalcher, I.; Dzubiella, J. NaCl crystallization in apolar nanometer-sized confinement studied by atomistic simulations. *Phys. Rev. E* **2013**, *88*, No. 062312.

(8) Gladkov, S. O. On Mathematical Description of Crystallization as a Deterministic Chaos Problem. *Tech. Phys.* **2008**, *53*, 952−955.

(9) Komatsuzaki, T.; Berry, R. S. Chemical reaction dynamics: Many-body chaos and regularity. *Adv. Chem. Phys.* **2003**, *123*, 79−152.

(10) Zheng, H.; Smith, R. K.; Jun, Y.-w.; Kisielowski, C.; Dahmen, U.; Alivisatos, A. P. Observation of single colloidal platinum nanocrystal growth trajectories. *Science* **2009**, *324*, 1309−1312.

(11) Jonkheijm, P.; van der Schoot, P.; Schenning, A. P. H. J.; Meijer, E. W. Probing the solvent-assisted nucleation pathway in chemical self-assembly. *Science* **2006**, *313*, 80−83.

(12) Zhou, J.; Yang, Y.; Yang, Y.; Kim, D. S.; Yuan, A.; Tian, X.; Ophus, C.; Sun, F.; Schmid, A. K.; Nathanson, M.; Heinz, H.; An, Q.; Zeng, H.; Ercius, P.; Miao, J. Observing crystal nucleation in four dimensions using atomic electron tomography. *Nature* **2019**, *570*, 500−503.

(13) Zeng, Z.; Zheng, W.; Zheng, H. Visualization of colloidal nanocrystal formation and electrode-electrolyte interfaces in liquids using TEM. *Acc. Chem. Res.* **2017**, *50*, 1808−1817.

(14) Durán-Olivencia, M. A.; Lutsko, J. F. Mesoscopic nucleation theory for confined systems: A one-parameter model. *Phys. Rev. E* **2015**, *91*, No. 022402.

(15) Wallace, A. F.; Hedges, L. O.; Fernandez-Martinez, A.; Raiteri, P.; Gale, J. D.; Waychunas, G. A.; Whitelam, S.; Banfield, J. F.; De Yoreo, J. J. Microscopic evidence for liquid-liquid separation in supersaturated CaCO$_3$ solutions. *Science* **2013**, *341*, 885−889.

(16) Grzybowski, B. A.; Winkleman, A.; Wiles, J. A.; Brumer, Y.; Whitesides, G. M. Electrostatic self-assembly of macroscopic crystals using contact electrification. *Nat. Mater.* **2003**, *2*, 241−245.

(17) Girard, M.; Wang, S.; Du, J. S.; Das, A.; Huang, Z.; Dravid, V. P.; Lee, B.; Mirkin, C. A.; de la Cruz, M. O. Particle analogs of electrons in colloidal crystals. *Science* **2019**, *364*, 1174−1178.

(18) Harano, K.; Homma, T.; Niimi, Y.; Koshino, M.; Suenaga, K.; Leibler, L.; Nakamura, E. Heterogeneous nucleation of organic crystals mediated by single-molecule templates. *Nat. Mater.* **2012**, *11*, 877−881.

(19) Xing, J.; Schweighauser, L.; Okada, S.; Harano, K.; Nakamura, E. Atomistic Structures and Dynamics of Prenucleation Clusters in MOF-2 and MOF-5 Syntheses. *Nat. Commun.* **2019**, *10*, 3608.

(20) Isobe, H.; Tanaka, T.; Maeda, R.; Noiri, E.; Solin, N.; Yudasaka, M.; Iijima, S.; Nakamura, E. Preparation, purification, characterization, and cytotoxicity assessment of water-soluble, transition-metal-free carbon nanotube aggregates. *Angew. Chem., Int. Ed.* **2006**, *45*, 6676−6680.

(21) Shimizu, T.; Lungerich, D.; Stuckner, J.; Murayama, M.; Harano, K.; Nakamura, E. Real-time video imaging of mechanical motions of a single molecular shuttle with sub-millisecond sub-angstrom precision. *Bull. Chem. Soc. Jpn.* **2020**, *93*, 1079−1085.

(22) Kvashnin, A. G.; Sorokin, P. B.; Yakobson, B. I. Flexoelectricity in Carbon Nanostructures: Nanotubes, Fullerenes, and Nanocones. *J. Phys. Chem. Lett.* **2015**, *6*, 2740−2744.

(23) Liao, H.-G.; Zherebetskyy, D.; Xin, H.; Czarnik, C.; Ercius, P.; Elmlund, H.; Pan, M.; Wang, L.-W.; Zheng, H. Facet development during platinum nanocube growth. *Science* **2014**, *345*, 916−919.

(24) Saiki, K. Fabrication and characterization of epitaxial films of ionic materials. *Appl. Surf. Sci.* **1997**, *113/114*, 9−17.

(25) Siwick, B. J.; Dwyer, J. R.; Jordan, R. E.; Miller, R. J. D. An atomic-level view of melting using femtosecond electron diffraction. *Science* **2003**, *302*, 1382−1385.

(26) Nakamura, E. Atomic-resolution transmission electron microscopic movies for study of organic molecules, assemblies, and reactions: The first 10 years of development. *Acc. Chem. Res.* **2017**, *50*, 1281−1292.

(27) Okada, S.; Kowashi, S.; Schweighauser, L.; Yamanouchi, K.; Harano, K.; Nakamura, E. Direct microscopic analysis of individual C$_{60}$ dimerization events: Kinetics and mechanisms. *J. Am. Chem. Soc.* **2017**, *139*, 18281−18287.

(28) Nakamura, E.; Harano, K. Chemical kinetics study through observation of individual reaction events with atomic-resolution electron microscopy. *Proc. Jpn. Acad., Ser. B* **2018**, *94*, 428−440.

(29) Recent review; Sandoval, S.; Tobias, G.; Flahaut, E. Structure of inorganic nanocrystals confined within carbon nanotubes. *Inorg. Chim. Acta* **2019**, *492*, 66−75.

(30) Hanayama, H.; Yamada, J.; Harano, K.; Nakamura, E. Cyclodextrins as surfactants for solubilization and purification of carbon nanohorn aggregates. *Chem. - Asian J.* **2020**, *15*, 1549−1552.

(31) Barrett, W. T.; Wallace, W. E. Studies of NaCl-KCl solid solutions. I. Heats of formation, lattice spacings, densities, Schottky defects and mutual solubilities. *J. Am. Chem. Soc.* **1954**, *76*, 366−369.

(32) Lai, J.; Lu, X.; Zheng, L. Convergence from clusters to the bulk solid: An *ab initio* investigation of clusters Na$_n$Cl$_n$ (n = 2−40). *PhysChemComm* **2002**, *5*, 82−87.

(33) Cowley, J. M.; Iijima, S. Electron Microscope Image Contrast for Thin Crystals. *Z. Naturforsch., A: Phys. Sci.* **1972**, *27a*, 445−451.

(34) Pflaum, R.; Sattler, K.; Recknagel, E. Multiphoton stimulated desorption: the magic numbers of neutral sodium chloride clusters. *Chem. Phys. Lett.* **1987**, *138*, 8−12.